Aberrant MNX1 expression associated with t(7;12)(q36;p13) pediatric acute myeloid leukemia induces the disease through altering histone methylation

Ahmed Waraky,[1,2] Anders Östlund,[1] Tina Nilsson,[2] Dieter Weichenhan,[3] Pavlo Lutsik,[3] Marion Bähr,[3] Joschka Hey,[3] Gürcan Tunali,[1] Jenni Adamsson,[1] Susanna Jacobsson,[2] Mohammad Hamdy Abdelrazak Morsy,[1] Susann Li,[2] Linda Fogelstrand,[1,2] Christoph Plass[3] and Lars Palmqvist[1,2]

[1]Department of Laboratory Medicine, Institute of Biomedicine, University of Gothenburg, Gothenburg, Sweden; [2]Department of Clinical Chemistry, Sahlgrenska University Hospital, Gothenburg, Sweden and [3]Division of Cancer Epigenomics, German Cancer Research Center (DKFZ), Heidelberg, Germany

Correspondence: L. Palmqvist
lars.palmqvist@clinchem.gu.se

Received: October 9, 2022.
Accepted: June 5, 2023.
Early view: June 15, 2023.

https://doi.org/10.3324/haematol.2022.282255

Abstract

Certain subtypes of acute myeloid leukemia (AML) in children have inferior outcome, such as AML with translocation t(7;12)(q36;p13) leading to an *MNX1::ETV6* fusion along with high expression of MNX1. We have identified the transforming event in this AML and possible ways of treatment. Retroviral expression of MNX1 was able to induce AML in mice, with similar gene expression and pathway enrichment to t(7;12) AML patient data. Importantly, this leukemia was only induced in immune incompetent mice using fetal but not adult hematopoietic stem and progenitor cells. The restriction in transforming capacity to cells from fetal liver is in alignment with t(7;12)(q36;p13) AML being mostly seen in infants. Expression of MNX1 led to increased histone 3 lysine 4 mono-, di- and trimethylation, reduction in H3K27me3, accompanied with changes in genome-wide chromatin accessibility and genome expression, likely mediated through MNX1 interaction with the methionine cycle and methyltransferases. MNX1 expression increased DNA damage, depletion of the $Lin^-/Sca1^+/c\text{-}Kit^+$ population and skewing toward the myeloid lineage. These effects, together with leukemia development, were prevented by pre-treatment with the S-adenosylmethionine analog Sinefungin. In conclusion, we have shown the importance of MNX1 in development of AML with t(7;12), supporting a rationale for targeting MNX1 and downstream pathways.

Introduction

Non-random cytogenetic aberrations are often involved in the development of acute myeloid leukemia (AML) and several aberrations can serve as diagnostic markers, prognosis predictors, and impact the choice of therapy.[1] In AML diagnosed in children under the age of 24 months, a chromosomal translocation t(7;12)(q36;p13) with poor prognosis has been reported.[2] There have been contradictory results on the incidence of t(7;12), but recent studies suggest the frequency in children <24 months to be 5-7%.[3,4] Similarly, different results have been reported regarding the prognosis, where recent studies show 20-43% 3-year event-free survival but with a high relapse rate, ranging from 57% to 80%.[3,4] However, the mechanisms behind the leukemia transformation of t(7;12) AML remain poorly understood.

The chromosomal break points in t(7;12) have consistently been found to be located close to the motor neuron and pancreas homeobox 1 (*MNX1*) gene on chromosome 7, and in introns 1 or 2 in the *ETV6* gene in chromosome 12.[5] The translocation leads to *MNX1* gene activation, and in most reported cases also to an *MNX1::ETV6* fusion transcript consisting of exon1 of *MNX1* transcript variant 1 spliced to the remaining ETV6 exons, depending on the location of the break point in ETV6.[6]

MNX1, also known as Homeobox HB9 (*HLXB9*), belongs to the homeobox domain family of transcription factors, with previous studies showing the importance of MNX1 in motor neuron development,[7] pancreas development,[8,9] and in hereditary sacral agenesis.[10] *ETV6*, also known as *TEL*, belongs to the ETS-family transcription factors. *ETV6* encodes a transcriptional repressor that plays a critical role in embryonic development and hematopoiesis, where it is essential for normal hematopoietic stem cell function and the generation of thrombocytes by megakaryocytes.[11]

Translocations involving the chromosomal region of 12p13

that result in the rearrangements of the *ETV6* gene are one of the most observed chromosomal abnormalities in human leukemia, with more than 30 reported translocations. These chromosomal translocations can induce leukemias through the ectopic expression of a proto-oncogene in the vicinity of a chromosomal translocation[12] or the constitutive activation of the partner protein.[13] In addition, the formation of ETV6 fusion proteins can result in the modification of the original functions of the transcription factor,[14] or loss of function of the fusion gene, affecting *ETV6* and the partner gene.[15]

The role of the MNX1::ETV6 fusion protein in the development of AML with t(7;12) has not been established. It is also unclear whether the driver of leukemogenesis is the MNX1::ETV6 fusion protein or overexpression of MNX1. The aim of this study was to assess the transformation capacity and the molecular mechanism of the MNX1::ETV6 fusion and the ectopic expression of MNX1 *in vitro* and *in vivo* using murine transplantation models.

Methods

Plasmid constructions

The *MNX1*, *ETV6* and *MNX1::ETV6* fusion sequences are listed in *Online Supplementary Table S1*. An HA-tag (36bp) is introduced at the 5' end and via a linker sequence of 24 bp attached to the separate gene sequences where the first ATG is removed. These constructs were cloned into the MSCV-IRES-GFP and MSCV-IRES-YFP vectors (Takara, Japan) #634401 under control of the viral LTR promoter.

Generation of transduced murine bone marrow cells and transplantation assays

Mice were bred and maintained at the Gothenburg University Laboratory for Experimental Biomedicine Animal Facility (Gothenburg, Sweden) in a specific pathogen-free environment. Establishment and characterization of bone marrow (BM) cell lines following transduction of BM cells with *MNX1*, *MNX1::ETV6*, *ETV6* or empty vector Control (Ctrl) were performed as described previously.[16] In brief, BM cell lines were established from BM cells previously treated with 5-fluorouracil (5-FU) from 8-12-week old (C57Bl/6) mice (Charles River Laboratories Inc., Wilmington, MA, USA) for three days for adult bone marrow (ABM) or from fetal liver at embryonic days 14.5 (E14.5) and maintained in liquid culture (Dulbecco's modified Eagle's medium supplemented with 18% fetal bovine serum, 10 ng/mL human interleukin [IL]-6, 6 ng/mL murine IL-3, and 50 ng/mL murine stem cell factor). All culture media were obtained from Sigma and recombinant growth factors from Peprotech. To generate *MNX1*, *MNX1::ETV6*, *ETV6* or empty vector Ctrl BM cell lines, the BM cells were transduced by co-cultivation on irradiated (4000 cGy) E86 producers (ATCC, Manassas, VA, USA) for a period of two days in the presence of 5 μg/mL protamine sulfate (Sigma). Cells were sorted for GFP^+ and/or YFP^+ expression by flow cytometry analysis (fluorescence-activated cell sorting [FACS]) FACSAria (BD Biosciences) and maintained in culture for 5-7 days post transduction before transplantation in mice. Lethally (8.5 Gy) or sublethally (5.5 Gy) radiated 8-12-week old C57Bl/6 mice received the equivalent of $0.6x10^6$ rescue BM cells and/or $0.8\text{-}1x10^6$ transduced cells via tail vein injection. For immunocompromised NOD.Cg-*Kit*$^{W\text{-}41J}$ *Tyr*$^{+}$ *Prkdc*^{scid} *Il2rg*^{tm1Wjl}/ThomJ (NBSGW) mice (The Jackson Laboratory, Bar Harbor, ME, USA), cells were transplanted either with no radiation, or after lethal dose (1.6 Gy) and sublethal dose (0.9 Gy). Donor-derived engraftment and reconstitution were monitored by flow cytometry analysis for GFP^+ and/or YFP^+ expression in the peripheral blood of the transplants every two weeks. Mice were sacrificed using isoflurane (Baxter, Deerfield, IL, USA). Blood counts were analyzed on a Sysmex KX-21 Hematology Analyzer (Sysmex, Norderstedt, Germany).

Statistical analysis

Two-sided Student's *t* test were used for comparisons between different groups in all experiments, unless stated otherwise. Log-rank test was used to compare survival between mice groups. Mann-Whitney two-tailed U-test was used for comparison between t(7;12) patients and normal human bone marrow from Target cohort.

Complete methods are available in the *Online Supplementary Appendix.*

Ethics statement

All animal experiments have been accepted by the Swedish Agency for Agriculture (Jordbruksverket) and the animal ethics committee in Gothenburg: Dnr 5.8.18-17008/2021.

Results

MNX1 induces acute myeloid leukemia in hematopoietic cells of fetal origin

To investigate the leukemogenic potential of t(7;12), we transduced primary murine (C57BL/6) hematopoietic stem and progenitor cells (HSPC) from either adult BM after 5-FU stimulation (ABM-HSPC) or fetal liver cells at E14.5 (FL-HSPC) with retroviral vectors for expression of the *MNX1::ETV6* fusion, *MNX1*, *ETV6* or empty vector (Ctrl). Expression of *MNX1*, *ETV6* and *MNX1::ETV6* was confirmed in both FL-HSPC and ABM-HSPC (*Online Supplementary Figure S1A-C*). The transduced cells were transplanted into lethally irradiated C57BL/6 mice with rescue BM. Neither *MNX1* overexpression nor *MNX1::ETV6* in ABM-HSPC or FL-HSPC were able to induce leukemia in these mice, as assessed by survival, white blood cell (WBC) count, hemoglobin, blood smears, and spleen size (*Online Sup-*

plementary Figure S2A-D). However, when increasing the percentage of *MNX1* chimerism through sublethal radiation with no rescue BM, 20% of the mice exhibited signs of malignant transformation after transplantation with FL-HSPC, including high WBC count, severe anemia, and enlarged spleen (*Online Supplementary Figure S2E, F* and *3A, B*). To further examine the leukemogenic potential of *MNX1* overexpression and the *MNX1::ETV6* fusion, we repeated the experiment using immune-compromised non-irradiated NOD.Cg-*Kit*$^{W\text{-}41J}$ *Tyr*$^{+}$ *Prkdc*^{scid} *Il2rg*^{tm1Wjl}/ThomJ (NBSGW) mice. Within 12-18 weeks after transplant, the MNX1 mice showed clear signs of leukemia, including pallor, weight loss, severe anemia, leukocytosis with a high percentage of *MNX1*-transduced cells, elevated blast cells in blood and BM, enlarged spleen, and liver infiltrated by leukemia (Figure 1A-D). Cells from BM showed predominant expression of the c-Kit protein, but not the stem cell marker SCA-1 or more differentiated myeloid markers such as Mac-1, Ly6G1 and Ly6C1, suggesting a poorly differentiated myeloid leukemia (Figure 1D, *Online Supplementary Figures S3D* and *S4A)*. To rule out the possibility that the leukemia development in immunocompromised mice was due to enhanced transplantation efficiency, we reduced the chimerism of *MNX1* cells in NBSGW mice through the usage of lethal radiation and rescue BM. These mice also developed leukemia but with a slightly longer latency than mice that were sublethally irradiated without rescue BM (*Online Supplementary Figure S3D*). Acute leukemia induction by MNX1 was confirmed by leukemia development after secondary transplant of BM from mice with primary leukemia, both in non-irradiated mice and in sublethally irradiated mice receiving rescue BM (*Online Supplementary Figure S5A*). When NBSGW mice were transplanted with ABM-HSPC transduced with *MNX1*, there were no signs of leukemia six months after the transplant (Figure 1E, *Online Supplementary Figure S5C, D*). Taken together, leukemogenesis was achieved by MNX1 only in the immunocompromised setting with fetal origin of leukemic cells.

MNX1 alters differentiation in favor of myeloid lineage while increasing proliferation and colony replating capacity of the cells

In order to characterize this leukemia model, *in vitro* FL-HSPC (r-FL) transduced with *MNX1::ETV6*, *MNX1*, *ETV6* or empty retroviral vector control were assessed for their immunophenotype. Both *MNX1* and *MNX1::ETV6* altered differentiation in favor of myeloid lineage, with *MNX1* showing the most prominent effects. *MNX1* increased Mac-1 and Ly6C^{+} cells, accompanied by depletion of the Lin^{-}/Sca1^{+}/c-kit^{+} (LSK) population, while *MNX1::ETV6* only increased Ly6C^{+} cells (Figure 2A, B, *Online Supplementary Figure S4B-D*). Ectopic expression of MNX1 reduced the progenitor MEP population without significantly affecting CMP or GMP (*Online Supplementary Figure S5A*). In addition, MNX1 increased GEMM colonies with a concomitant reduction in BFU colonies and increased both CFU replating and proliferation capacity (Figure 2C, D, *Online Supplementary Figure S6F-H*). In ABM-HSPC *in vitro* cells (r-ABM), *MNX1* had similar effects but to a lower extent, and *MNX1::ETV6* fusion had no effect (*Online Supplementary Figure S6C-E*).

MNX1 induces DNA damage

To investigate the molecular pathway through which MNX1 is mediating its leukemogenic effect, differential gene expression between *MNX1* FL-HSPC leukemic NSG BM cells and FL-HSPC transduced with empty vector (Ctrl) was assessed with RNA-sequencing (RNA-Seq) (Figure 2E, *Online Supplementary Figure S7*). Gene Ontology (GO) biological pathway and gene set enrichment (GSEA) analyses revealed that the highest enriched pathways in *MNX1* cells involved DNA damage, cell cycle, chromatin organization, methylation of histones, metabolic processes, megakaryocyte and myeloid cell differentiation pathways (Figure 2E). Similar results were seen when using BM taken from mice transplanted with FL-HSPC with empty vector as Control (*Online Supplementary Figure S8*). The effect on DNA damage was confirmed through examination of γH2AX foci induction. MNX1, and to a lower extent MNX1::ETV6, induced a higher number of γH2AX foci, indicative of higher DNA damage, in *in vitro* FL-HSPC as well as in ABM-HSPC (r-Fl and r-ABM) (Figure 3A, B, *Online Supplementary Figure S9A, B*). In both *MNX1* and *MNX1::ETV6* transduced FL-HSPC (r-FL), the DNA damage was accompanied with a transient G1 cell cycle accumulation and fewer cells in S-phase (Figure 3C, *Online Supplementary Figure S9C*). No such effect was observed in ABM-HSPC (r-ABM), where the G1 cells were replaced by a Sub-G1 peak suggestive of apoptotic cells after 3-4 weeks of transduction (*Online Supplementary Figure S9D*). Using Annexin-V and DAPI staining, a 3.5-4-fold increase in apoptosis was induced by MNX1 in ABM-HSPC (r-ABM), but not in FL-HSPC (r-FL) (Figure 3D, E). Following up the consequences of such pronounced DNA damage, we showed that BM from NSG leukemia mice exhibited an increase in the amount of DNA or a hyperploidy in comparison with the BM from Ctrl mice as indicated by increased DNA index (*Online Supplementary Figure S10A, B*). An interesting candidate for mediating DNA damage identified in several differentially regulated pathways was the centrosomal protein 164 (*Cep164*) (*Online Supplementary Table S2*). Increased expression of *Cep164* was confirmed with qPCR in both *MNX1* transduced FL-HSPC and leukemia BM (*Online Supplementary Figure S10C*). Furthermore, MNX1 increased binding to the promoter of *Cep164* was detected by ChIP-qPCR (*Online Supplementary Figure S10C*), along with altered binding of histone modifications that can change *CEP164* expression, namely H3K4me3 and H3K27me3 in the same promoter region (*Online Supplementary Figure S10D*).

MNX1 alters histone modifications globally affecting chromatin accessibility

Since MNX1 induced histone modifications H3K4me3 and H3K27me3 at the *Cep164* promoter, we assessed global histone modifications. Western blotting showed altered H3K4me3, H3K27me3, and both mono- and di-methylation of the H3K4 *in vitro* and in BM from NSG leukemic mice (Figure 4A, *Online Supplementary Figure S10E*). Co-immunoprecipitation experiments (Co-IP) confirmed the association of MNX1 to histone H3 (*Online Supplementary Figure S11A*). Antibody-guided chromatin tagmentation sequencing (ACT-Seq) was then used for mapping genome-wide distribution of the histone modifications (Figure 4B). H3K27me3 histone modification showed fewer accessible

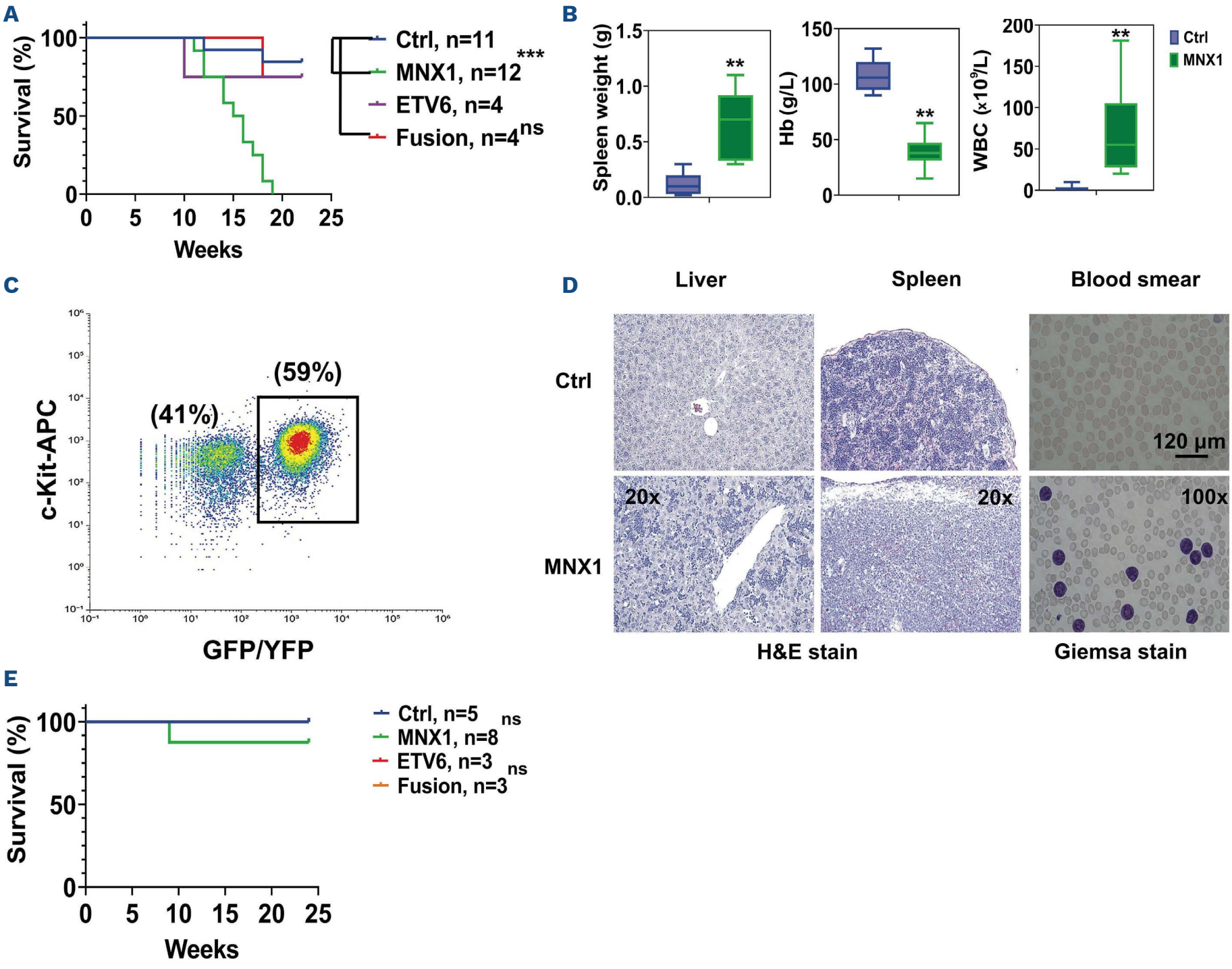

Figure 1. MNX1 induces acute myeloid leukemia in immunocompromised mice. (A) Kaplan-Meier survival curve of immunocompromised NOD.Cg-*Kit*$^{W\text{-}41J}$ *Tyr*$^{+}$ *Prkdc*^{scid} *Il2rg*^{tm1Wjl}/ThomJ (NBSGW) mice transplanted with fetal liver hematopoietic stem and progenitor cells after retrovirus transduction (r-FL-HSPC) with either ectopic expression of *MNX1* (green), *ETV6* (purple), *MNX1::ETV6* fusion (red), or empty vector control (Ctrl) (blue). Results from the transplanted mice (control N=11, *MNX1*: N=12, *ETV6* and *MNX1::ETV6* N=4) were analyzed using the log-rank test: ***P≤0.01; ns: not significant. (B) Mice were euthanized when showing sign of disease or at the end of the experiment, and analyzed for spleen weight (g), white blood cell (WBC) count, and hemoglobin concentration (Hb). (C) Quantification of flow cytometry analysis of bone marrow (BM) cells from (NBSGW) mice with c-Kit expression showing all events. Green fluorescence protein (GFP) / yellow fluorescence protein (YFP) were used as indicative for MNX1 expression. (D, left) Representative images of Hematoxylin & Eosin (H&E)-stained formaldehyde fixed liver and spleen sections from Ctrl and MNX1 mice. (D, right) Representative images of Giemsa-stained peripheral blood smears from Ctrl and MNX1 mice. (E) Kaplan-Meier survival curves of NBSGW mice transplanted with adult bone marrow (ABM) cells with either ectopic expression of *MNX1*, *ETV6*, *MNX1::ETV6* fusion or Ctrl after sub-lethal radiation (0.9 Gy) with no rescue BM. Results of Ctrl and transfected mice (Ctrl N= 5, *MNX1* N=8, *ETV6* and *MNX1::ETV6* N=3) were analyzed using the log-rank test (ns: not significant). Data represent mean ± Standard Deviation of at least three experiments. Two-sided student *t* test: **P≤0.01; *P≤0.05; ns: not significant at P>0.05. Fusion: *MNX1::ETV6* fusion; LSK: Lin^{-}Sca^{-}1+c-Kit^{+}; NSG: NOD.Cg-*Kit*$^{W\text{-}41J}$ *Tyr*$^{+}$ *Prkdc*^{scid} *Il2rg*^{tm1Wjl}/ThomJ (NBSGW).

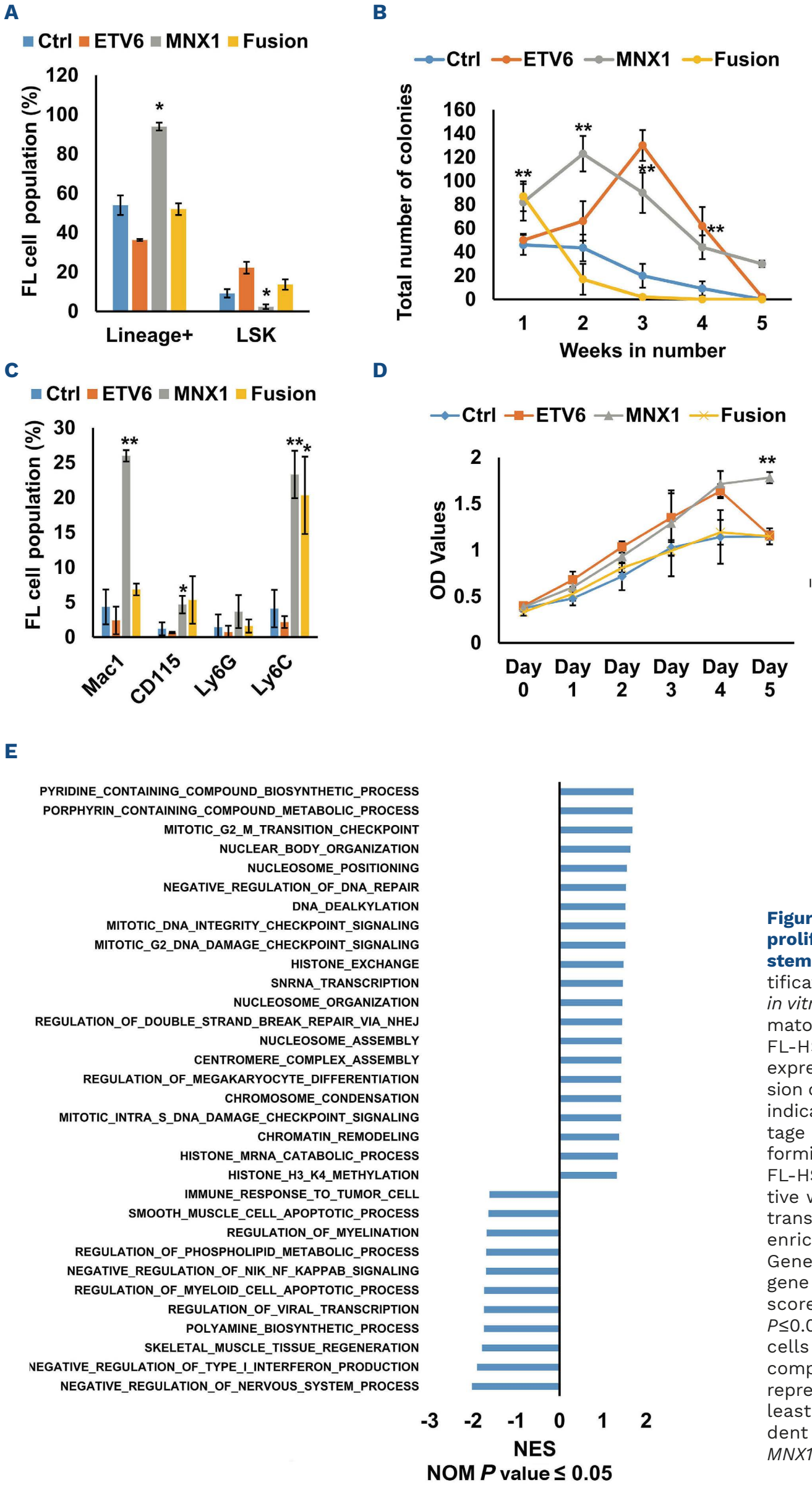

Figure 2. MNX1 alters differentiation and proliferation of fetal liver hematopoietic stem and progenitor cells. (A and B) Quantification of the flow cytometry analysis of *in vitro* retroviral transduced fetal liver hematopoietic stem and progenitor cells (r-FL-HSPC) cells transduced with ectopic expression of *MNX1*, *ETV6*, *MNX1::ETV6* fusion or empty vector control (Ctrl) with the indicated antibodies presented as percentage of population. (C) Number of colony forming unit colonies after transduction of FL-HSPC with replating for five consecutive weeks. (D) MTT proliferation assay of transduced *in vitro* r-FL cells. (E) Gene set enrichment analysis (GSEA) using the Gene Ontology (GO) biological pathways gene set showing normalized enrichment score (NES) (nominal *P* value [NOM]: $P \leq 0.05$) for pathways from leukemia BM cells with *MNX1* ectopic expression in comparison with FL-HSPC with Ctrl. Data represent mean ± Standard Deviation of at least three experiments. Two-sided student *t* test: $^{**}P \leq 0.01$; $^{*}P \leq 0.05$. Fusion: *MNX1::ETV6* fusion; LSK: $Lin^{-}Sca^{-}1^{+}c\text{-}Kit^{+}$.

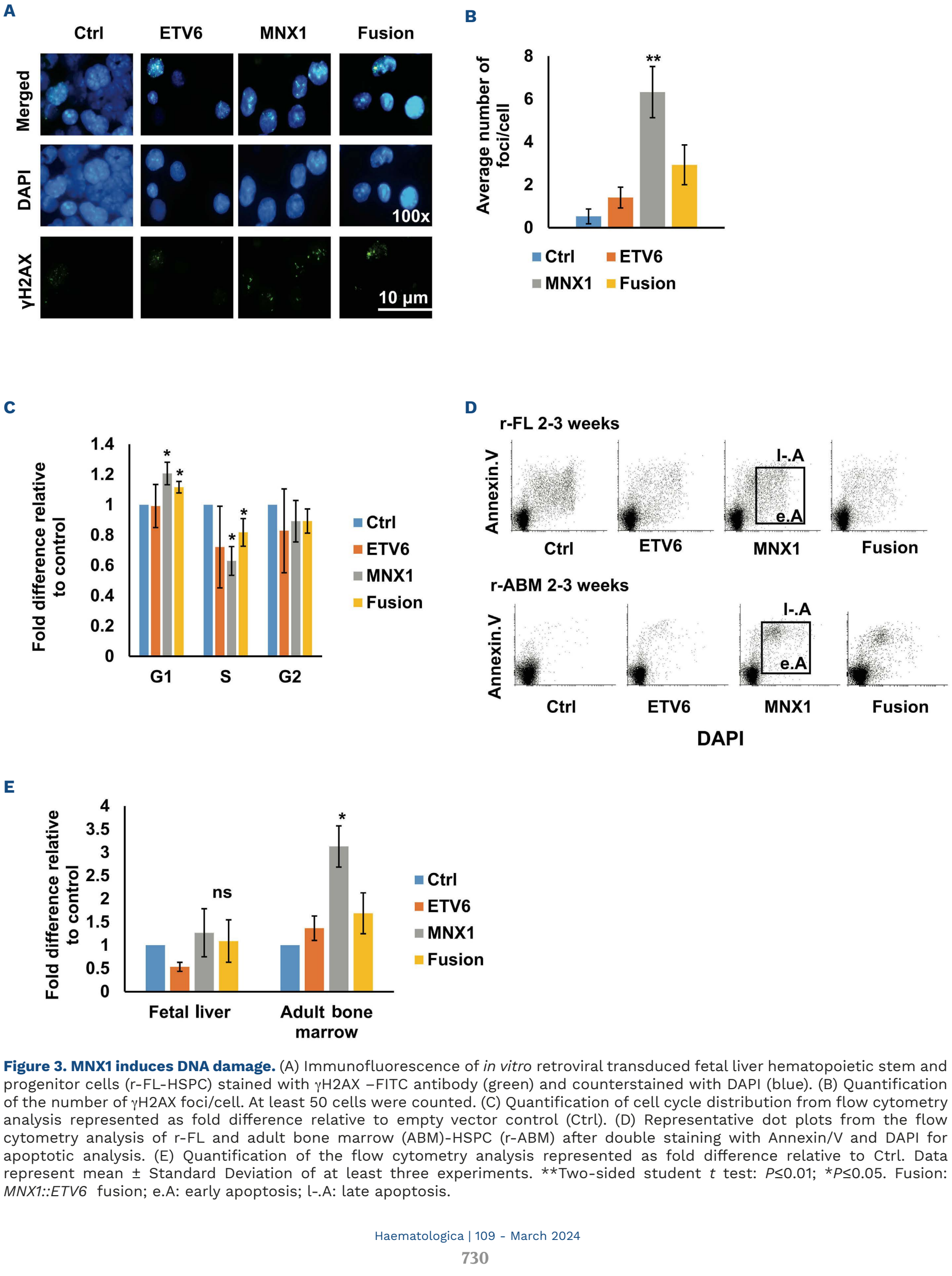

Figure 3. MNX1 induces DNA damage. (A) Immunofluorescence of *in vitro* retroviral transduced fetal liver hematopoietic stem and progenitor cells (r-FL-HSPC) stained with γH2AX –FITC antibody (green) and counterstained with DAPI (blue). (B) Quantification of the number of γH2AX foci/cell. At least 50 cells were counted. (C) Quantification of cell cycle distribution from flow cytometry analysis represented as fold difference relative to empty vector control (Ctrl). (D) Representative dot plots from the flow cytometry analysis of r-FL and adult bone marrow (ABM)-HSPC (r-ABM) after double staining with Annexin/V and DAPI for apoptotic analysis. (E) Quantification of the flow cytometry analysis represented as fold difference relative to Ctrl. Data represent mean ± Standard Deviation of at least three experiments. **Two-sided student *t* test: $P \leq 0.01$; *$P \leq 0.05$. Fusion: *MNX1::ETV6* fusion; e.A: early apoptosis; l-.A: late apoptosis.

regions in MNX1 (BM from NSG leukemic mice) compared to Ctrl (FL-HSPC transduced with empty vector) (False Discovery Rate [FDR] ≤ 0.05, log2 fold change ≥ 1), involving mainly distal intergenic regions followed by promoter and other intronic regions (Figure 4B). The consequences of these histone modifications on chromatin accessibility were investigated with ATAC-Seq. MNX1 leukemic BM cells exhibited increased number of accessible chromatin regions in MNX1 (BM from NSG leukemic mice) compared to Ctrl (FL-HSPC transduced with empty vector) (FDR ≤ 0.05, log2 fold change ≥ 1) (Figure 4C), mainly involving promoters, followed by distal intergenic and intronic regions, very similar to the pattern seen for H3K27me3 (Figure 4B). Pathway analysis of genes annotated to the differentially accessible regions from ATAC-Seq (FDR ≤ 0.05, log2 fold change ≥ 1) revealed similar enrichment to the RNA-Seq, with high enrichment in metabolic pathways, myeloid cell

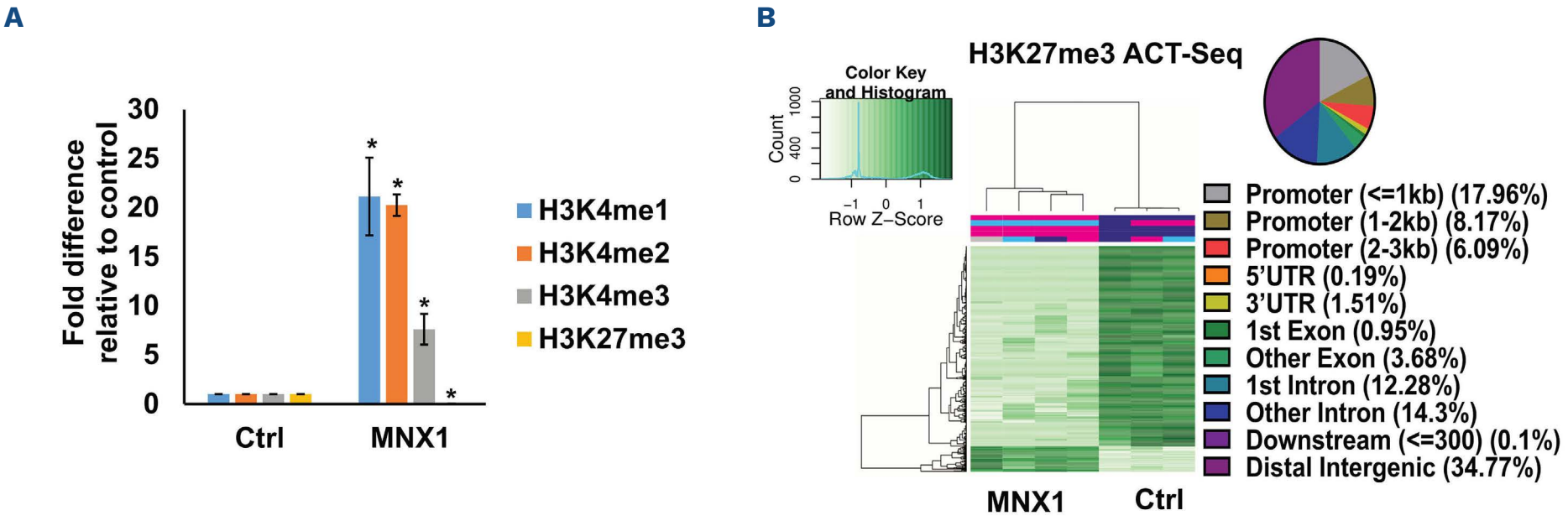

Figure 4. MNX1 alters histone methylation. (A) ImageJ quantification of western blot analysis of H3K4me1, H3K4me2, H3K4me3, and H3K27me3 as fold difference relative to loading control. (B) Heatmap of differentially bound H3K27me3 from bone marrow (BM) of leukemic mice (MNX1) *versus* control fetal liver hematopoietic stem and progenitor cells (FL-HSPC) transduced with empty vector (Ctrl) as determined by ACT-Seq and annotation of different enriched regions for H3K27me3 ACT-Seq. Results were considered at the log fold-change cut-off (logFC) of ≥ |1| and false discovery rate (FDR) of ≤0.05. (C) Heatmap of differentially accessible regions from BM of leukemic mice (MNX1) *versus* control FL-HSPC transduced with Ctrl as determined by ATAC-Seq and annotation of different enriched regions for ATAC-Seq. Results were considered at the log fold-change cut-off (logFC) of ≥ |1| and false discovery rate (FDR) of ≤0.05. (D) Scatter plot showing the correlation between differentially expressed genes from RNA-Seq expression analysis and genes with differentially accessible regions from ATAC-Seq analysis. Results were considered at the log fold-change cut-off (logFC) of ≥ |1| and FDR of ≤0.05. AML: acute myeloid leukemia.

differentiation, erythrocyte differentiation, cytoskeleton organization, cell cycle process, and apoptotic cell process (*Online Supplementary Figure S11B*). Further analysis through integrating ATAC-Seq data with *in silico* predicted transcription factor binding sites by DiffTF package, revealed 130 differentially activated sites (FDR < 0.05) between MNX1 leukemic BM cells and Ctrl FL-HSPC (Table 1, *Online Supplementary Figure S11C*). These were enriched in pathways of myeloid/erythrocyte differentiation, cellular metabolism, G1/S-phase transition of cell cycle, histone methylation, DNA methylation and DNA damage response (Table 1, *Online Supplementary Figure S11C*). A significant correlation between the accessible chromatin regions identified by ATAC-Seq and differentially expressed genes by RNA-Seq was shown at r_s=0.47 and (P≤0.01) (Figure 4D). In conclusion, MNX1 induces global histone modifications that are affecting chromatin accessibility and inducing differential gene regulation.

MNX1 alters the methylation of histone H3

To understand the mechanism for the MNX1-induced global histone modifications, we performed mass spectrometry analysis to study proteins in association with MNX1. FL-HSPC cells were transduced with retroviral *MNX1* with a HA-tag and MNX1-associated proteins were co-immunoprecipitated using anti-HA antibody. Pathway analysis using STRING for protein-protein interactions for the identified proteins revealed a high enrichment for methylation pathway proteins MAT2A, MAT2B and AHCY (Table 2, Figure 5A), in addition to several S-adenosylmethionine (SAM)-dependent methyl transferases and their downstream targets (*Online Supplementary Table S3*). Co-IP confirmed the association of MNX1 to MAT2A and AHCY both *in vitro* and in NSG BM leukemic cells (Table 1, Figure 5B, *Online Supplementary Figure S12A*), with no effect on protein expression as shown in parallel with western blot (*Online Supplementary Figure S12B*). Furthermore, MNX1 overexpression increased the concentration of S-adenosylhomocysterin (SAH) and reduced free methionine in both FL cells and leukemia NSG BM cells (*Online Supplementary Figure S12C-E*). In support of an MNX1 role in methylation pathway and in altering histone methylation, MNX1 pulled down with Co-IP and incubated with recombinant Histone H3 resulted in methylation of Histone H3 (Figure 5C, D, *Online Supplementary Figure S12F, G*).

MNX1-induced leukemia in mice and in human pediatric t(7;12) acute myeloid leukemia show similar gene expression and pathway enrichment

To validate the similarity between the AML developed in our mouse model with human t(7;12) AML, we used our RNA-Seq data on leukemic cells from mice and retrieved RNA-Seq data from pediatric t(7;12) AML patient samples from the Children's Oncology Group (COG)-National Cancer Institute (NCI) TARGET AML initiative data set. Differential gene expression in mouse leukemia was determined by comparing *MNX1* FL-HSPC leukemic NSG BM cells and FL-HSPC transduced with empty vector, and differential gene expression in human AML was determined by comparing pediatric t(7;12) AML patient samples with normal human BM. Comparing the differential gene expression between the mouse AML with MNX1 expression and the t(7;12) patient data revealed close to 50% overlapping differential gene expression (Figure 5E, *Online Supplementary Table S4*). These included increased expression of the genes *MNX1*, *cKIT*, *CEP164*, *AHCY*, *MAT2A*

Table 1. *In silico* predicted transcription factor binding sites by DiffTF package from ATAC-Seq showing top differentially activated (False Discovery Rate < 0.05) transcription factors binding between MNX1 bone marrow from leukemia mice and fetal liver hematopoietic stem and progenitor cell Control cells.

Up-regulated TF	Weighted mean difference	Adj *P*	Down-regulated TF	Weighted mean difference	Adj *P*
Tal1.a	1.294844532	9.30E-79	Fosl2	-0.421333369	1.84E-24
Gata1	0.567577232	1.24E-20	Jun	-0.415408916	2.58E-23
Gata3	0.550998432	1.12E-19	Cebpe	-0.39280302	0.000108
Gata2	0.540274293	1.01E-16	Batf	-0.387629056	1.57E-17
Alx1	0.371423122	0.023026	Fosl1	-0.384618862	4.57E-21
Nf2l2	0.288226747	2.11E-17	Cebpa	-0.353311343	3.14E-06
Zeb1	0.232871599	9.60E-41	Gfi1	-0.349686909	8.73E-08
Tbx5	0.231419764	1.76E-09	Fosb	-0.339609157	5.76E-15
Mafk.s	0.22701829	3.01E-10	Sta5a	-0.339203846	2.94E-09
Nfe2	0.218904994	4.77E-11	Jund	-0.337147615	8.92E-16
Gata6	0.213067314	2.28E-11	Cebpd	-0.323368792	0.000182
Foxo3	0.202788032	0.000274	Gfi1b	-0.308823273	8.94E-12

TF: transcription factors; Adj P: adjusted *P* value.

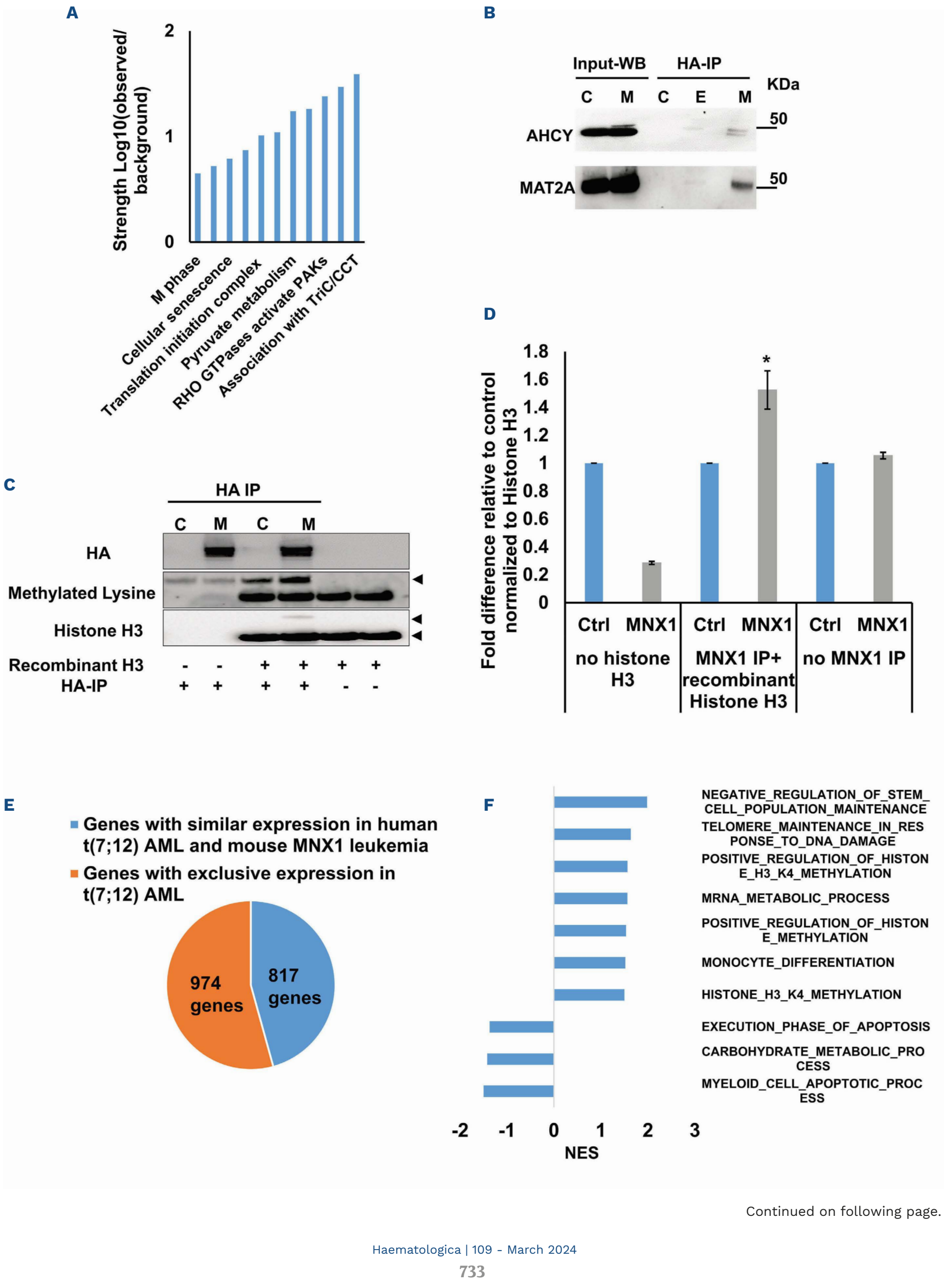

Continued on following page.

Figure 5. MNX1 associates with proteins from the methionine cycle and show similar gene expression and pathway enrichment with human t(7;12) acute myeloid leukemia. (A) Pathway enrichment analysis for the identified proteins after co-immunoprecipitation experiments (Co-IP) and mass spectrometry using STRING with reactome data set, showing strength of the pathway as Log10 observed proteins/background in the respective pathway. (B) Binding of AHCY and MAT2A was detected by immunoprecipitation (IP) of MNX1 using HA-antibody followed by western blot (WB) using AHCY and MAT2A antibodies. ETV6 with HA tag was used as a negative control. Total protein input used as loading control (Ctrl). (C) Recombinant Histone H3.1and H3.3 were subjected to an *in vitro* methyltransferase reaction using MNX1 complex pulled down with HA antibody from FL-HSPC transduced with MNX1 (M), in comparison with fetal liver hematopoietic stem and progenitor cells (FL-HSPC) with empty vector control (Ctrl), in the presence of S-adenosylmethionine (SAM) and dithiothreitol (DTT). The reactions were terminated by boiling in SDS sample buffer. Separation of samples in 12% SDS-PAGE was followed by immunoblotting (IB) with mono-, di- and trimethyl-lysines antibody. Reblotting was made for detection of HA and total Histone H3. As indicated, negative controls were obtained by omitting Histone H3, or the pulled down immune complex. (D) Quantification of the *in vitro* methyltransferase reaction. Data represent mean ± Standard Deviation of at least three experiments. Two-sided student *t* test: $^{**}P \leq 0.01$; $^{*}P \leq 0.05$. (E) Graph showing differentially expressed genes with same or opposite regulation when comparing gene expression data from t(7;12) acute myeloid leukemia (AML) patients from the TARGET database and RNA-seq data from bone marrow (BM) from mice with MNX1-induced leukemia. Differentially expressed genes were selected based on a LogFC ±1 and false discovery rate ≤ 0.05. Gene set enrichment analysis (GSEA) using the Gene Ontology (GO) biological pathways, showing normalized enrichment score (NES) for common pathways between t(7;12) AML patients and the MNX1-induced leukemia in mice with nominal *P* value (NOM) $P \leq 0.05$.

and *MAT2B* (*Online Supplementary Figure S13*). Pathway enrichment analysis of the t(7;12) patient using GSEA revealed several common enriched pathways including: DNA damage, H3K4methylation, monocyte differentiation, apoptotic processes, and metabolic processes (Figure 5F, *Online Supplementary Figure S14A*). Interestingly, only the H3K4me3 methylation, and no other histone methylation pathway, was enriched in the GSEA analysis from t(7;12) AML patients. In addition, we analyzed the global methylation on H3K4me3 in a human t(7;12) iPSC-derived model. These cells show high expression of MNX1 when differentiated into HSPC, but also manifest other important features seen in human t(7;12) AML.[17] This model gave similar results with increased methylation of H3K4me3 in t(7;12) iPSC differentiated into HSPC compared to the parental iPSC differentiated into HSPC without t(7;12) (*Online Supplementary Figure S14B, C*), thus, highlighting the biological significance of high MNX1 expression also in human cells with t(7;12).

The effects of MNX1 on methylation are crucial for leukemogenesis

To confirm the importance of this effect for MNX1-induced leukemia, we used the natural nucleoside analog of SAM, sinefungin, which acts as a competitor and accordingly a pan-methyltransferase inhibitor.[18] Adding 5 μM of sinefungin to MNX1-transduced FL-HSPC partially or completely prevented the effects of MNX1 on histone modifications (Figure 6A, *Online Supplementary Figure S15A*), DNA damage induction (Figure 6B, *Online Supplementary Figure S15B*), cell cycle distribution (*Online Supplementary Figure S15C*), myeloid differentiation, and LSK depletion (Figure 6C, D). Furthermore, when MNX1 FL-HSPC was pre-treated *in vitro* with sinefungin and then transplanted into NBSGW mice, there were no signs of leukemia development (Figure 6E, *Online Supplementary Figure S15D, E*), despite maintained high *MNX1* expression (*Online Supplementary Figure S15F*) and continuous presence of viable transplanted cells in blood (*Online Supplementary Figure S16A*). To investigate the effect of sinefungin treatment on MNX1-induced differential gene expression, RNA-Seq was performed before and after treatment. Differentially expressed genes (FDR ≤ 0.05, log2 fold change ≥ 1.5) from MNX1 cells after treatment (MNX+S) clustered with MNX1 (Figure 6F), and most of the differentially expressed genes by MNX1 overexpression remained at a similar level after treatment (Figure 6F), with a limited number of genes altered in MNX1 differential gene expression after treatment (*Online Supplementary Figure S16B*).

Discussion

The t(7;12) has only been reported in children diagnosed with AML before the age of 24 months. The function of this translocation in inducing infant leukemia and the reason for its absence in adult leukemia is unknown. In the current study using a murine model, we showed that ectopic expression of MNX1 rather than the *MNX1::ETV6* fusion was able to initiate and drive leukemogenesis. Our data suggest a mechanism through which MNX1 is mediating the leukemogenic effect through aberrant methylation that results in histone modifications and DNA damage.

The malignant transformation mediated by MNX1 overexpression in our mouse model matched the criteria for AML,[19] compatible with an AML without maturation. This mouse MNX1-driven leukemia had a high degree of differentially-expressed gene that overlaps with the gene expression signature and pathway enrichment that is seen in human AML with t(7;12). It has also been shown that MNX1 clearly has oncogenic properties in both human and murine hematopoietic cells by inducing a myeloid biased perturbed hematopoietic differentiation and premature senescence.[20] This fits well with the properties seen in our mouse leukemia model with both a block in differentiation

Table 2. Identified proteins in top enriched pathways after co-immunoprecipitation experiments of proteins in complex with MNX1 and mass spectrometry analysis, as determined by STRING using reactome data set.

Pathway	Matching proteins
Association with TriC/CCT	Cct8, Cct6a, Tcp1, Cct4
Methylation	Mat2b, Ahcy, Mat2a, Trmt112
RHO GTPases activate PAK	Ppp1cb, Myh9, Myh11, Myh10, Myh14
Citric acid cycle (TCA cycle)	Cs, Mdh2, Idh3g, Dld
Pyruvate metabolism	Pdk3, Slc16a3, Vdac1, Ldha, Dld
Actin dynamics for phagocytic	Actr2, Arpc2, Myh9, Cyfip2, Arpc3, Myo5a, Actr3
Translation initiation complex	Pabpc1, Eif3e, Rps21, Eif2s3x, Rps12, Rps28
RHO GTPase effectors	Actr2, Mapk14, Arpc2, Ppp1cb, Myh9, Pfn1, Aurkb, S100a8, Tuba1b, Bub3, Myh11, Cyfip2, Arpc3, Myh10, Ywhaq, Myh14, Kif2a, S100a9, Actr3
Cellular senescence	Mapk14, Asf1a, Lmnb1, Txn1, H2afz, Hist1h1b, Hist2h2be, Eed
Mitotic anaphase	Psmd11, Aurkb, Psmd6, Lmnb1, Smc3, Psmd13, Chmp4b, Smc1a, Tuba1b, Rcc1, Bub3, Kif2a
M phase	Psmd11, Aurkb, Psmd6, Lmnb1, Smc3, Psmd13, Chmp4b, H2afz, Smc1a, Smc4, Tuba1b, Rcc1, Bub3, Hist2h2be, Csnk2a1, Smc2, Kif2a
Metabolism of proteins	Pabpc1, Srp14, Psmd11, Rab10, Ddx5, Aurkb, Psmd6, Vdac2, Ero1l, Eif3e, Mrpl21, Smc3, Psmd13, Cct8,Srp9, Txn1, Trappc3, Cct6a, Cmas, Rab27a, Rpl22l1, Smc1a, Rpl37, Mat2b, Pdia6, Fn1, Rps21, Eif2s3x, Hist2h2ab, Rps12, Tuba1b, Ctbp1, Rpl15, Rpl36, Rpl34, Lgals1, Hist2h2be, Eef1g, Csnk2a1, Vdac1, Wdr5, Rps28, Trmt112, Tcp1, Copa, Gnb4, Ctsd, Cct4, Nop58, Tceb1
Metabolism of RNA	Pabpc1, U2af2, Psmd11, Prpf8, Snrpd3, Ddx5, Psmd6, Wdr46, Psmd13, Rpl22l1, Rpl37, Utp15, Wdr43, Rps21, Rcl1, Rps12, Rpl15, Rpl36, Rpl34, Srsf2, Nhp2l1, Snrpb, Rps28, Srsf3, Ddx6, Hnrnpd, Apobec3, Nop58

and induced cell cycle arrest. Similar gene expression and pathway enrichment has also been shown between human cells with an engineered t(7;12) translocation, which results in high expression of MNX1, and human t(7;12) AML, suggesting a common gene expression program induced by MNX1 in hematopoietic cells.[17,21] Our data showed that ectopic expression of MNX1 was able to induce AML using HSPC from fetal origin but not from adult BM. One possible reason for this was the dramatic induction of apoptosis seen in the hematopoietic progenitor cells from adult BM, prohibiting leukemic transformation. The higher susceptibility for apoptosis and DNA damage induced by MNX1 is concordant with the presence of naturally occurring DNA damage in the adult stem cells.[22] Possibly, the balance between fetal and adult stem cell programs affects the transforming ability of the cells upon overexpression of MNX1. Lin28b has been shown to be a key regulator of the self-renewing capacity characteristic of fetal, but not adult, hematopoietic stem cells.[23] *LIN28B* is, together with *MNX1*, a signature gene expressed in all pediatric t(7;12) AML and not seen in other AML subtypes.[24] Lin28b was seen expressed in our MNX1-induced mouse leukemia (*Online Supplementary Table S2*), which suggests that transformation by MNX1 might be dependent on Lin28b for its transforming effects or, and perhaps more likely, indicates that the fetal hematopoietic program is needed for MNX1 oncogenesis. However, the expression of *Lin28b* in our leukemia and *LIN28B* in human t(7;12) AML contrasts with the finding that Lin28b suppresses MLL-ENL fusion-driven leukemogenesis, also typically seen in infant leukemia.[25] But what is intriguing is that, in adult mice, the potential of an MLL-ENL fusion to initiate leukemia development peaks during neonatal development and then drops dramatically.[25] The importance of the development stage of cells that can be transformed into leukemia, including the leukemia phenotype as well as intrinsic properties of progenitor populations have been shown in several studies.[26-28] Other factors that differ between fetal and adult hematopoietic stem cells and that might affect their propensity for transformation are metabolic demand and cell cycle profile.[29-31] Even though MNX1 overexpression induced leukemia in the cells of fetal origin, the fusion *MNX1::ETV6* by itself did not induce leukemia. This finding is in line with the previously reported inability

to induce transformation with *MNX1::ETV6* (HLXB9/TEL) *in vitro* and the paucity of transgenic mouse models of AML with *MNX1::ETV6*.[32] In our study, the development of leukemia induced by MNX1 expression was primarily seen in immunocompromised NSG mice. Thus, the adaptive B- and T-cell immune response might be enough to eradicate cells with overexpression of MNX1 and prevent leukemia development. This may be yet another clue to how AML with t(7;12) develops in very young children, typically before six months of age when the immune system is still under development.[4-6]

Our studies of MNX1 expression *in vitro* revealed an in-

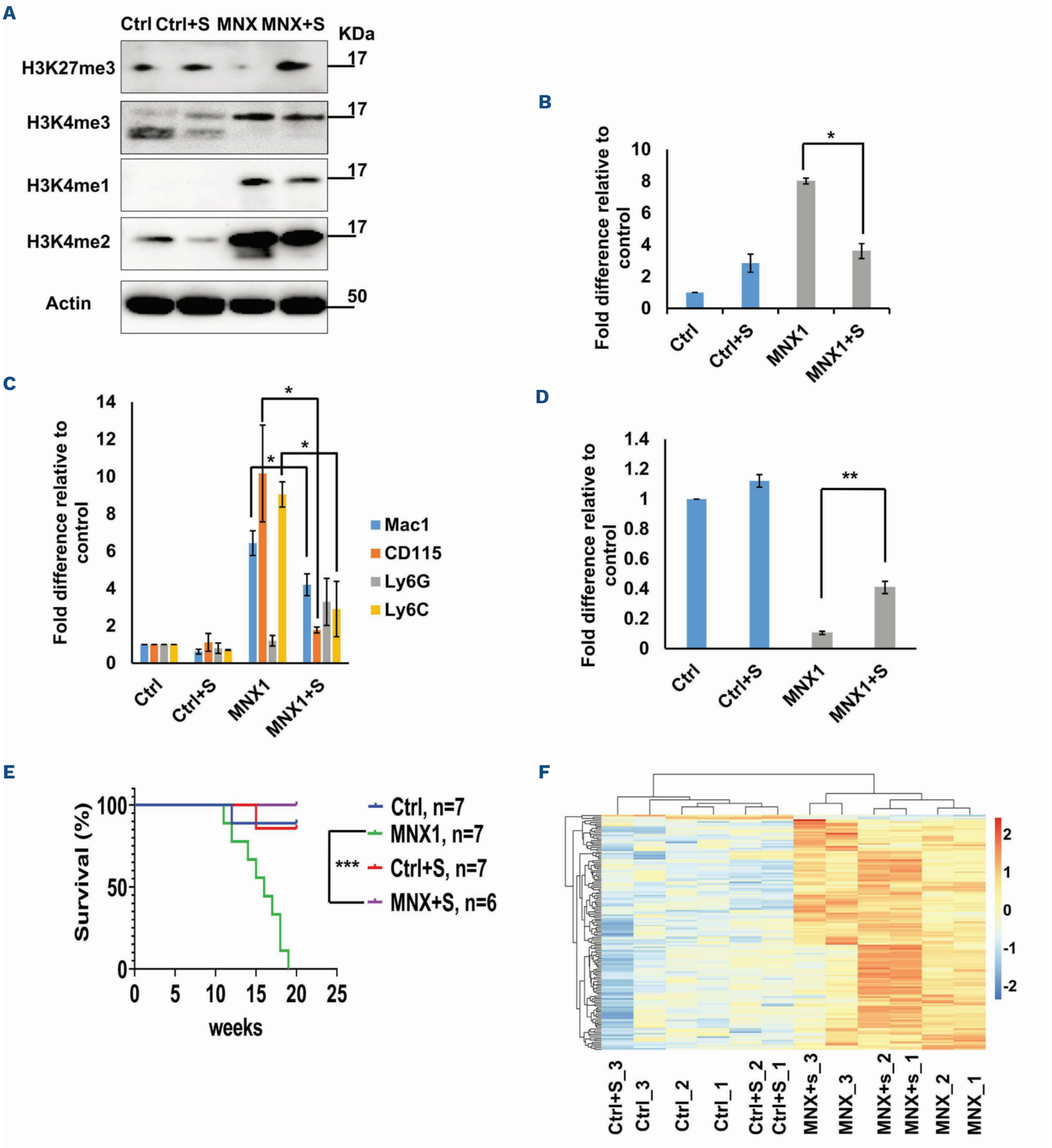

Continued on following page.

Figure 6. Sinefungin rescued MNX1-induced phenotype. (A) Protein expression levels of H3K4me3, H3k27me3, H3K4me1 and H3K4me2 in *in vitro* retroviral induced fetal liver hematopoietic stem and progenitor cells (r-FL-HSPC) with either MNX1 overexpression or empty vector (Ctrl) after treatment with vehicle or 5 μM sinefungin (Ctrl+S, MNX1+S) as determined by western blotting. Actin served as loading control. (B) Quantification of the western blot analysis in *Online Supplementary Figure S9A*. Quantification of the number of γH2AX foci/cell. At least 50 cells were counted. Data represented as fold difference relative to control. (C and D) Quantification of flow cytometry analysis of the cells with the indicated antibodies. Data represented as fold difference relative to control. Data represent mean ± Standard Deviation of at least three experiments. Two-sided Student *t* test between MNX1 and MNX1+S: ***P*≤0.01; **P*≤0.05. (E) Kaplan-Meier survival curves of (NBSGW) mice transplanted with FL cells after retrovirus transduction with either ectopic expression of MNX1 or Ctrl after treatment with vehicle or 5 μM sinefungin (MNX1+S, Ctrl+S). Results of MNX1 (N=7) and sinefungin-treated MNX1 cells (MNX1+S) (N=6) were analyzed using the log-rank test: ****P*≤0.01. (F) LogFC heat map of down-regulated (blue) and up-regulated (red) differentially expressed genes of FL cells with *MNX1* ectopic expression (MNX) in comparison with FL cells with Ctrl, with 5 μM sinefungin (Ctrl+S, MNX+S) or without treatment (Ctrl, MNX1), showing clustering and similarity between the samples. Results were considered at the log fold-change cut-off (LogFC) ≥ |1.5| and false discovery rate ≤ 0.05.

duction of DNA damage both in FL-HSPC and ABM-HSPC, which could contribute to the observed skewed differentiation towards myeloid lineage evident by the depletion of LSK and MEP population and increased $Mac1^+$ and $Ly6C^+$ populations. The influence of DNA damage in stem cells on differentiation was first demonstrated in melanocyte stem cells, where ionizing radiation triggered differentiation into mature melanocytes.[33] In hematopoietic stem cells, DNA damage can induce differentiation towards lymphoid or myeloid lineage, and may be the reason for the skewing towards myeoloid differentiation in the aging hematopoietic system.[34-37]

We found MNX1 to associate with members of the methionine cycle, including MAT2A, AHCY and MAT2B, in addition to several downstream SAM-dependent methyl transferases. Methionine is an essential amino acid that is converted to the universal methyl donor SAM, which is converted to SAH upon the donation of its methyl group. This reaction is catalyzed by methionine adenosyl transferases (MAT). SAM is used as a co-factor in most methylation reactions and provides the activated methyl group for methylation of proteins, including histones, DNA, RNA, and lipids. These methylation events are highly dependent on methionine metabolism, with alterations in methionine showing profound effects on DNA and histone methylation.[38,39] The role of another homeodomain protein (MSX1) in recruiting methyltransferase to regulate gene expression and chromatin structure through histone modifications has been shown in the differentiation of myoblasts.[40,41] During neural development, MNX1 binding to loci on chromatin is enriched for H3K4me1 and H3K4me3.[42] Therefore, the binding and association of MNX1 with methyltranferases and members of the methionine cycle, and the subsequent change in chromatin structure and histone modifications, might represent the physiological role for MNX1 during differentiation.[43,44] We conclude that the abnormal expression of MNX1 and subsequent effect on the methionine cycle and chromatin structure in hematopoietic cells acts as the driver of leukemia transformation, supported by the inhibition of the phenotype by the SAM analog sinefungin.

In conclusion, our results provide the biological and clinical significance for MNX1 as an epigenetic regulator in pediatric t(7;12) AML. Given that many epigenetic modifications are chemically reversible, the inhibition of MNX1 ectopic expression or its downstream effects in t(7;12) could provide a foundation for alternative treatment options to improve outcome.

Disclosures

No conflicts of interest to disclose.

Contributions

LP, AÖ and AW designed the research study. AW, AÖ, TN, DW, PL, JH, JA, SL, GT, SJ and MHM performed the laboratory work and results analysis. AW, LF, CP and LP analyzed the combined data and wrote the paper.

Acknowledgments

We thank Mohamad Ali and Akram Mendez for help with bioinformatic analysis and Tova Johansson and Hanna Brissman for help with animals.

Funding

This work was supported by grants from the Swedish Cancer Society (20 0925 PjF, CAN2017/461), the Swedish Childhood Cancer Foundation (PR2014-0125, PR2019-0013 and TJ2019-0053, TJ2022-0017), Wilhelm och Martina Lundgrens Fond, Assar Gabrielsson Fond and Västra Götalandsregionen (ALFGBG-431881), and the German Funding Agency (DFG) with funding for Collaborative Research Center 1074, Project B11N (to CP). The computations were enabled by resources in project SNIC 2021/22-754 provided by the Swedish National Infrastructure for Computing (SNIC) at UPPMAX, partially funded by the Swedish Research Council through grant agreement n. 2018-05973.

Data-sharing statement

The data that support the findings of this study are available in the Online Supplementary Appendix of this article, from Gene Expression Omnibus (GEO) database, accession number GSE182168, GSE202137 and GSE205698, and from PRIDE/ProteomeXchange, accession number PDXD034416. Further details and other data that support the findings of this study are available from the corresponding author upon request.

References

1. Lagunas-Rangel FA, Chavez-Valencia V, Gomez-Guijosa MA, Cortes-Penagos C. Acute myeloid leukemia-genetic alterations and their clinical prognosis. Int J Hematol Oncol Stem Cell Res. 2017;11(4):328-339.
2. von Bergh AR, van Drunen E, van Wering ER, et al. High incidence of t(7;12) (q36;p13) in infant AML but not in infant ALL, with a dismal outcome and ectopic expression of HLXB9. Genes Chromosomes Cancer. 2006;45(8):731-739.
3. Bolouri H, Farrar JE, Triche T Jr, et al. The molecular landscape of pediatric acute myeloid leukemia reveals recurrent structural alterations and age-specific mutational interactions. Nat Med. 2018;24(1):103-112.
4. Espersen ADL, Noren-Nystrom U, Abrahamsson J, et al. Acute myeloid leukemia (AML) with t(7;12)(q36;p13) is associated with infancy and trisomy 19: Data from Nordic Society for Pediatric Hematology and Oncology (NOPHO-AML) and review of the literature. Genes Chromosomes Cancer. 2018;57(7):359-365.
5. Beverloo HB, Panagopoulos I, Isaksson M, et al. Fusion of the homeobox gene HLXB9 and the ETV6 gene in infant acute myeloid leukemias with the t(7;12) (q36;p13). Cancer Res. 2001;61(14):5374-5377.
6. Tosi S, Mostafa Kamel Y, Owoka T, Federico C, Truong TH, Saccone S. Paediatric acute myeloid leukaemia with the t(7;12)(q36;p13) rearrangement: a review of the biological and clinical management aspects. Biomark Res. 2015;3:2.
7. Thaler J, Harrison K, Sharma K, Lettieri K, Kehrl J, Pfaff SL. Active suppression of interneuron programs within developing motor neurons revealed by analysis of homeodomain factor HB9. Neuron. 1999;23(4):675-687.
8. Li H, Arber S, Jessell TM, Edlund H. Selective agenesis of the dorsal pancreas in mice lacking homeobox gene Hlxb9. Nat Genet. 1999;23(1):67-70.
9. Harrison KA, Thaler J, Pfaff SL, Gu H, Kehrl JH. Pancreas dorsal lobe agenesis and abnormal islets of Langerhans in Hlxb9-deficient mice. Nat Genet. 1999;23(1):71-75.
10. Ross AJ, Ruiz-Perez V, Wang Y, et al. A homeobox gene, HLXB9, is the major locus for dominantly inherited sacral agenesis. Nat Genet. 1998;20(4):358-361.
11. Hock H, Shimamura A. ETV6 in hematopoiesis and leukemia predisposition. Semin Hematol. 2017;54(2):98-104.
12. Rawat VP, Cusan M, Deshpande A, et al. Ectopic expression of the homeobox gene Cdx2 is the transforming event in a mouse model of t(12;13)(p13;q12) acute myeloid leukemia. Proc Natl Acad Sci U S A. 2004;101(3):817-822.
13. Golub TR, Barker GF, Lovett M, Gilliland DG. Fusion of PDGF receptor beta to a novel ets-like gene, tel, in chronic myelomonocytic leukemia with t(5;12) chromosomal translocation. Cell. 1994;77(2):307-316.
14. Zelent A, Greaves M, Enver T. Role of the TEL-AML1 fusion gene in the molecular pathogenesis of childhood acute lymphoblastic leukaemia. Oncogene. 2004;23(24):4275-4283.
15. De Braekeleer E, Douet-Guilbert N, Morel F, Le Bris MJ, Basinko A, De Braekeleer M. ETV6 fusion genes in hematological malignancies: a review. Leuk Res. 2012;36(8):945-961.
16. Arabanian LS, Johansson P, Staffas A, et al. The endothelin receptor type A is a downstream target of Hoxa9 and Meis1 in acute myeloid leukemia. Leuk Res. 2018;75:61-68.
17. Nilsson T, Waraky A, Ostlund A, et al. An induced pluripotent stem cell t(7;12) (q36;p13) acute myeloid leukemia model shows high expression of MNX1 and a block in differentiation of the erythroid and megakaryocytic lineages. Int J Cancer. 2022;151(5):770-782.
18. Zhang J, Zheng YG. SAM/SAH analogs as versatile tools for SAM-dependent methyltransferases. ACS Chem Biol. 2016;11(3):583-597.
19. Kogan SC, Ward JM, Anver MR, et al. Bethesda proposals for classification of nonlymphoid hematopoietic neoplasms in mice. Blood. 2002;100(1):238-245.
20. Ingenhag D, Reister S, Auer F, et al. The homeobox transcription factor HB9 induces senescence and blocks differentiation in hematopoietic stem and progenitor cells. Haematologica. 2019;104(1):35-46.
21. Ragusa D, Ciciro Y, Federico C, et al. Engineered model of t(7;12)(q36;p13) AML recapitulates patient-specific features and gene expression profiles. Oncogenesis. 2022;11(1):50.
22. Biechonski S, Yassin M, Milyavsky M. DNA-damage response in hematopoietic stem cells: an evolutionary trade-off between blood regeneration and leukemia suppression. Carcinogenesis. 2017;38(4):367-377.
23. Copley MR, Babovic S, Benz C, et al. The Lin28b-let-7-Hmga2 axis determines the higher self-renewal potential of fetal haematopoietic stem cells. Nat Cell Biol. 2013;15(8):916-925.
24. Balgobind BV, Van den Heuvel-Eibrink MM, De Menezes RX, et al. Evaluation of gene expression signatures predictive of cytogenetic and molecular subtypes of pediatric acute myeloid leukemia. Haematologica. 2011;96(2):221-230.
25. Okeyo-Owuor T, Li Y, Patel RM, et al. The efficiency of murine MLL-ENL-driven leukemia initiation changes with age and peaks during neonatal development. Blood Adv. 2019;3(15):2388-2399.
26. Ugale A, Norddahl GL, Wahlestedt M, et al. Hematopoietic stem cells are intrinsically protected against MLL-ENL-mediated transformation. Cell Rep. 2014;9(4):1246-1255.
27. Rowe RG, Lummertz da Rocha E, Sousa P, et al. The developmental stage of the hematopoietic niche regulates lineage in MLL-rearranged leukemia. J Exp Med. 2019;216(3):527-538.
28. Copley MR, Eaves CJ. Developmental changes in hematopoietic stem cell properties. Exp Mol Med. 2013;45(11):e55.
29. Manesia JK, Xu Z, Broekaert D, et al. Highly proliferative primitive fetal liver hematopoietic stem cells are fueled by oxidative metabolic pathways. Stem Cell Res. 2015;15(3):715-721.
30. Bowie MB, Kent DG, Dykstra B, et al. Identification of a new intrinsically timed developmental checkpoint that reprograms key hematopoietic stem cell properties. Proc Natl Acad Sci U S A. 2007;104(14):5878-5882.
31. Chen C, Yu W, Tober J, et al. Spatial genome re-organization between fetal and adult hematopoietic stem cells. Cell Rep. 2019;29(12):4200-4211.
32. Wildenhain S, Ruckert C, Rottgers S, et al. Expression of cell-cell interacting genes distinguishes HLXB9/TEL from MLL-positive childhood acute myeloid leukemia. Leukemia.

2010;24(9):1657-1660.
33. Inomata K, Aoto T, Binh NT, et al. Genotoxic stress abrogates renewal of melanocyte stem cells by triggering their differentiation. Cell. 2009;137(6):1088-1099.
34. Mandal PK, Rossi DJ. DNA-damage-induced differentiation in hematopoietic stem cells. Cell. 2012;148(5):847-848.
35. Beerman I, Bhattacharya D, Zandi S, et al. Functionally distinct hematopoietic stem cells modulate hematopoietic lineage potential during aging by a mechanism of clonal expansion. Proc Natl Acad Sci U S A. 2010;107(12):5465-5470.
36. Cho RH, Sieburg HB, Muller-Sieburg CE. A new mechanism for the aging of hematopoietic stem cells: aging changes the clonal composition of the stem cell compartment but not individual stem cells. Blood. 2008;111(12):5553-5561.
37. Scheffold A, Baig AH, Chen Z, et al. Elevated Hedgehog activity contributes to attenuated DNA damage responses in aged hematopoietic cells. Leukemia. 2020;34(4):1125-1134.
38. Kaiser P. Methionine dependence of cancer. Biomolecules. 2020;10(4):568.
39. Sanderson SM, Gao X, Dai Z, Locasale JW. Methionine metabolism in health and cancer: a nexus of diet and precision medicine. Nat Rev Cancer. 2019;19(11):625-637.
40. Wang J, Abate-Shen C. The MSX1 homeoprotein recruits G9a methyltransferase to repressed target genes in myoblast cells. PLoS One. 2012;7(5):e37647.
41. Wang J, Kumar RM, Biggs VJ, et al. The Msx1 homeoprotein recruits polycomb to the nuclear periphery during development. Dev Cell. 2011;21(3):575-588.
42. Sun M-A, Ralls S, Wu W, et al. Homeobox transcription factor MNX1 is crucial for restraining the expression of pan-neuronal genes in motor neurons. BioRxiv. 2021 Aug 7. doi: https://doi.org/10.1101/2021.08.07.455331 [preprint, not peer-reviewed].
43. Leotta CG, Federico C, Brundo MV, Tosi S, Saccone S. HLXB9 gene expression, and nuclear location during in vitro neuronal differentiation in the SK-N-BE neuroblastoma cell line. PLoS One. 2014;9(8):e105481.
44. Dalgin G, Ward AB, Hao le T, Beattie CE, Nechiporuk A, Prince VE. Zebrafish mnx1 controls cell fate choice in the developing endocrine pancreas. Development. 2011;138(21):4597-4608.